Communications

Electromagnetic Inverse Scattering of a Conducting Cylinder Buried in a Lossy Half-Space

Chien-Ching Chiu and Yean-Woei Kiang

Abstract—**The Newton-Kantorovitch algorithm is used to reconstruct the shape of a perfectly conducting cylinder buried in a lossy half-space from the measurement of scattered field along the interface. A typical example of the lossy half-space is the lossy underground with finite soil conductivity. After a brief description of the theoretical formulation, we concentrate on examining the effect of burying depth, soil conductivity and additive random noise on the quality of shape reconstruction. Numerical simulations show that the attenuation due to finite soil conductivity will deteriorate the image quality.**

I. Introduction

The electromagnetic inverse scattering of underground objects has attracted increasing attention due to interests in geophysical exploration and nondestructive evaluation. The development of practical numerical techniques for the inverse scattering problem of this type is important and urgent. One possible application is the detection of buried pipes and cables. However, the solutions are considerably more difficult than those involving objects in a free-space. This is due to the interaction between the air–earth interface and the object, which leads to the complicated Green's function for this half-space problem.

In the past few years, imaging for targets buried in a half-space has already been investigated by electromagnetic waves using either radar techniques [1] or holographic ones [2]. Another approach based on the diffraction tomography technique [3] has been applied to dielectric objects buried in the lossy soil. Chiu and Kiang [4] also rigorously solved the inverse scattering of a buried conducting cylinder by the Newton–Kantorovitch method, but only the case of a lossless half-space was treated in their numerical examples.

In this communication, which might be regarded as a continuation of [4], the inverse scattering of a perfectly conducting cylinder buried in a lossy half-space is numerically investigated. We analyze how the soil conductivity and burying depth influence the quality of shape reconstruction. In Section II, the theoretical formulation for the inverse scattering, which has been proposed in [4], is briefly described. Numerical results for objects of different shapes under the conditions of various burying depths, soil conductivities, and noise levels are given in Section III. Finally, some conclusions are drawn in Section IV.

Manuscript received May 14, 1991; revised June 12, 1992. This work was supported by the National Science Council, Republic of China, under Grant NSC 81-0404-E002-015.

C.-C. Chiu is with the Department of Electronic Engineering, Tamkang University, Taipei, Taiwan, Republic of China.

Y.-W. Kiang is with the Department of Electrical Engineering, National Taiwan University, Taipei 10764, Taiwan, Republic of China.

IEEE Log Number 9204897.

II. Theoretical Formulation

Let us consider a perfectly conducting cylinder buried in a lossy half-space (region 2) with permittivity ϵ_2 and conductivity σ_2, above which lies another half-space (region 1) with permittivity ϵ_1 and conductivity σ_1, as shown in Fig. 1. The permeability is that of the vacuum $\mu = \mu_0$ in each region. The axis of the buried cylinder is the z axis, and its cross section is described in polar coordinates in the xy plane by the equation $\rho = F(\theta)$, i.e., the object is of a star-like shape. It is then illuminated from the upper half-space by an incident plane wave whose electric field vector is parallel to the z axis (transverse magnetic or TM polarization). We assume that the time dependence of the field is harmonic with the factor $\exp(j\omega t)$. Let the incident field propagate from region 1 with incident angle ϕ_1. The unperturbed field, which would exist in the absence of the buried object, is then given by

$$E_i(x,y) = \begin{cases} E_1(x,y) = e^{-jk_1[x\sin\phi_1+(y+a)\cos\phi_1]} \\ \quad +R_1 e^{-jk_1[x\sin\phi_1-(y+a)\cos\phi_1]}, & y \le -a \\ E_2(x,y) = T_2 e^{-jk_2[x\sin\phi_2+(y+a)\cos\phi_2]}, & y > -a \end{cases}$$

where $k_i = \sqrt{\omega^2\epsilon_i\mu_0 - j\omega\mu_0\sigma_i}$, $\mathrm{Im}(k_i) \le 0$, $i = 1,2$, and constants R_1, T_2, and ϕ_2 are the reflection coefficient, transmission coefficient, and transmission angle, respectively.

At an arbitrary point (x, y) in the Cartesian coordinates or (r, θ) in the polar coordinates outside the scatterer, the scattered field E_s can be expressed by

$$E_s(x,y) = -\int_0^{2\pi} G(x,y;F(\theta'),\theta')J(\theta')\,d\theta' \qquad (1)$$

with

$$J(\theta) = -j\omega\mu_0\sqrt{F^2(\theta)+F'^2(\theta)}\,J_s(\theta). \qquad (2)$$

Here, $J_s(\theta)$ is the induced surface current density which is proportional to the normal derivative of the electric field on the conductor surface. G is the Green's function, which can be obtained by a Fourier transform [4]. The total tangential electric field is required to be zero on the surface of the scatterer to satisfy the boundary condition, and this then yields an integral equation for $J(\theta)$:

$$E_2(F(\theta),\theta) = \int_0^{2\pi} G(F(\theta),\theta;F(\theta'),\theta')J(\theta')\,d\theta'. \qquad (3)$$

Let us consider the following inverse problem: given the scattered field E_s measured in region 1, determine the shape function $F(\theta)$ of the object buried in region 2. The solution of

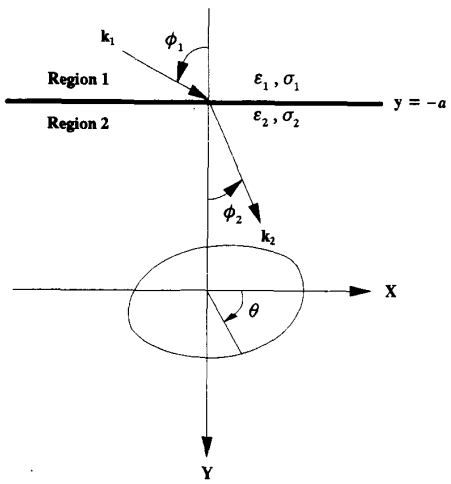

Fig. 1. Geometry of the problem in the (x, y) plane.

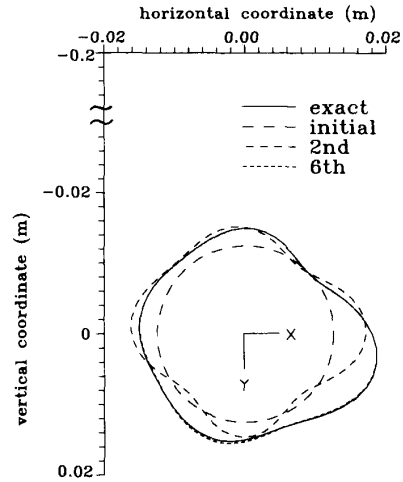

Fig. 2. Shape functions for object A buried in the soil ($\epsilon_2 = 2.55\epsilon_0$ and $\sigma_2 = 2 \times 10^{-2}$ S/m) at a depth of $a = 2\lambda_0$. The solid curve represents the exact profile, while the dashed curves are calculated profiles in the iteration process.

this inverse scattering is difficult because (1) and (3) depend nonlinearly on $F(\theta)$. In the inversion procedure, we first expand the shape function $F(\theta)$ as

$$F(\theta) \simeq \sum_{n=0}^{N/2} A_n \cos(n\theta) + \sum_{n=1}^{N/2} A'_n \sin(n\theta)$$

where A_n and A'_n are real coefficients to be determined. The Newton–Kantorovitch algorithm [4], [5] is then used to solve the nonlinear integral equations (1) and (3).

III. Numerical Simulations

Let us consider a perfectly conducting object buried in the soil, as shown in Fig. 1. An electromagnetic plane wave of unit amplitude is incident from region 1 upon the object, and the frequency of the incident wave is fixed at 3 GHz, i.e., the wavelength λ_0 is 0.1 m. The scattered field is measured on a probing line $y = -a$ along the interface between regions 1 and 2. The medium in region 1 is the air ($\epsilon_1 = \epsilon_0$ and $\sigma_1 = 0$). To reconstruct the shape of the cylinder, the object is illuminated by the incident waves from three different directions, and 20 measurement points at equal spacing are used along the interface $y = -a$ for each incident angle. There are totally 60 measurement points in each simulation. The measurement is taken from $x = 0$ to 0.2 m for incident angle $\phi_1 = -73^0$, from $x = -0.1$ to 0.1 m for incident angle $\phi_1 = 0^0$, and from $x = -0.2$ to 0 m for incident angle $\phi_1 = 73^0$. For numerical simulation, we first solve (3) by the method of moments, and generate the scattered field from (1) as exact synthetic data. Then the Newton–Kantorovitch algorithm is used to solve the inverse problem. Note that the number of unknown coefficients for expanding the shape function $F(\theta)$ is set to be nine (i.e., $N + 1 = 9$) in order to save computing time.

We now report on two objects of different shapes buried in various soils. In the first example, object A with shape function $F(\theta) = [0.015 + 7.5 \times 10^{-4}(\cos\theta + \cos 2\theta + \cos 3\theta + \cos 4\theta + \sin\theta + \sin 2\theta + \sin 3\theta + \sin 4\theta)]$ m is buried in the soil ($\epsilon_2 = 2.55\epsilon_0$ and $\sigma_2 = 2 \times 10^{-2}$ S/m) at a depth of $a = 2\lambda_0$. The reconstructed shape function is plotted in Fig. 2 . It is clear that the reconstruction on the back of the object is slightly less

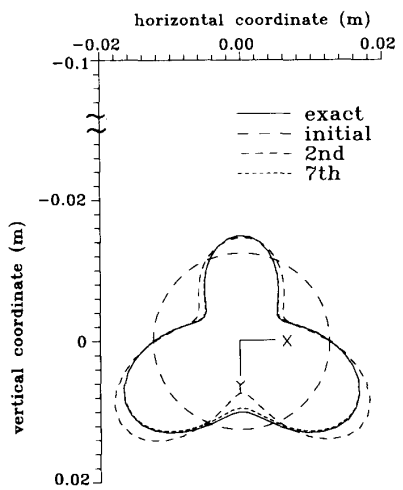

Fig. 3. Shape functions for object B buried in the sandy soil ($\epsilon_2 = 2.55\epsilon_0$ and $\sigma_2 = 2 \times 10^{-3}$ S/m) at a depth of $a = \lambda_0$. The solid curve represents the exact profile, while the dashed curves are calculated profiles in the iteration process.

accurate than that on the illuminated portion. In the second example, the shape function of object B is chosen as $F(\theta) = (0.0125 + 0.0025\sin\theta + 0.005\sin 3\theta)$ m. This object is buried in the sandy soil ($\epsilon_2 = 2.55\epsilon_0$ and $\sigma_2 = 2 \times 10^{-3}$ S/m) [3] at a depth of $a = \lambda_0$. The result is shown in Fig. 3 We can still see that reconstruction is quite good on the illuminated side, with a slight error on the backside.

Next, we investigate the reconstructed image of the object at different burying depths of $a = \lambda_0$, $a = 2\lambda_0$, and $a = 3\lambda_0$. Fig. 4 shows the reconstruction result of the objects buried in two different soils characterized by ($\epsilon_2 = 2.55\epsilon_0$, $\sigma_2 = 2 \times 10^{-3}$ S/m) and ($\epsilon_2 = 2.55\epsilon_0$, $\sigma_2 = 2 \times 10^{-2}$ S/m). The relative error means the error between the exact shape function and the

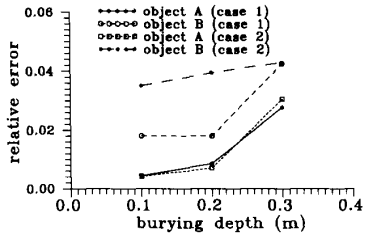

Fig. 4. Reconstruction error as a function of burying depth with two different soil parameters; case 1: ($\epsilon_2 = 2.55\epsilon_0$ and $\sigma_2 = 2 \times 10^{-3}$ S/m), case 2: ($\epsilon_2 = 2.55\epsilon_0$ and $\sigma_2 = 2 \times 10^{-2}$ S/m).

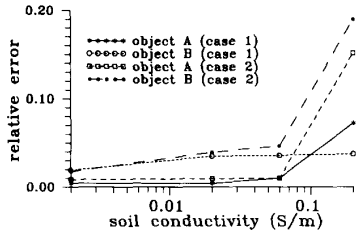

Fig. 5. Reconstruction error as a function of soil conductivity at two different burying depths; case 1: $a = \lambda_0$, case 2: $a = 2\lambda_0$.

calculated one in the root mean-square (rms) sense. In general, the larger the burying depth, the worse the image quality. This is due to the lossy character of the media and the limited length of the probing line. It is also observed that the reconstruction error is tolerable, even up to a burying depth of $3\lambda_0$. Moreover, the reconstruction error for object A is observed to be smaller than that for object B. This can be explained by the fact that the shape of object B is more complex and concave than that of object A.

The effect of the soil parameter on shape reconstruction is investigated below. Note that in all of the following examples, the soil permittivity is chosen to be $\epsilon_2 = 2.55\epsilon_0$. Four different soil conductivities $\sigma_2 = 2 \times 10^{-3}$ S/m, $\sigma_2 = 2 \times 10^{-2}$ S/m, $\sigma_2 = 6 \times 10^{-2}$ S/m, and $\sigma_2 = 2 \times 10^{-1}$ S/m are considered. Note that, in the case of normal incidence, the penetration depth is defined by $\delta = 1/|\mathrm{Im}(k_2)| = |\mathrm{Im}[\omega(\epsilon_2\mu_0)^{1/2}(1 - j(\sigma_2/\omega\epsilon_2))^{1/2}]|^{-1}$. The penetration depths corresponding to soil parameters ($\epsilon_2 = 2.55\epsilon_0$, $\sigma_2 = 2 \times 10^{-3}$ S/m), ($\epsilon_2 = 2.55\epsilon_0$, $\sigma_2 = 2 \times 10^{-2}$ S/m), ($\epsilon_2 = 2.55\epsilon_0$, $\sigma_2 = 6 \times 10^{-2}$ S/m), and ($\epsilon_2 = 2.55\epsilon_0$, $\sigma_2 = 2 \times 10^{-1}$ S/m) at 3 GHz are 4.24, 0.424, 0.142, and 0.043 m, respectively. The objects in Fig. 5 are buried at two different depths of $a = \lambda_0$ and $a = 2\lambda_0$. Numerical results show that the reconstruction error for small conductivity is less than that for large conductivity. Further, from Fig. 5, the reconstruction error seems intolerable for soil conductivity beyond 2×10^{-1} S/m. This is due to the fact that the burying depth is larger than the penetration depth, leading to high attenuation in the scattered field.

Now, we show how noise affects the reconstruction result for different soil conductivities. The random noise with uniform distribution ranging from a negative noise level to a positive noise level is independently added to both the real and imaginary parts of the scattered field. Note that in the following, all of the scattered fields and noise levels are normalized by the incident field. The noise levels used are 10^{-5}, 2×10^{-5}, 10^{-4}, 2×10^{-4}, and 10^{-3}. Object A is buried at a depth of $a = 2\lambda_0$ in three different kinds of soils. The parameters of the soils are ($\epsilon_2 = 2.55\epsilon_0$, $\sigma_2 = 2 \times 10^{-3}$ S/m), ($\epsilon_2 = 2.55\epsilon_0$, $\sigma_2 = 2 \times 10^{-2}$ S/m), and ($\epsilon_2 = 2.55\epsilon_0$, $\sigma_2 = 6 \times 10^{-2}$ S/m), respectively. Numerical results are plotted in Fig. 6. Note that the rms value of the scattered field is about 0.11, 4.84×10^{-2}, and 7.63×10^{-3}, corresponding to a soil conductivity of $\sigma_2 = 2 \times 10^{-3}$ S/m, $\sigma_2 = 2 \times 10^{-2}$ S/m, and $\sigma_2 = 6 \times 10^{-2}$ S/m, respectively. From Fig. 6, it is noticed that the reconstruction for $\sigma_2 = 6 \times 10^{-2}$ S/m is the worst, while the other two cases are acceptable at a noise level below 2×10^{-4}.

Finally, we reconstruct an object with the shape $F(\theta) = (0.005 + 0.001\sin\theta + 0.002\sin 3\theta)$ m buried in the loamy soil at a depth of $a = \lambda_0$. The loamy soil is characterized by $\epsilon_2 = 20\epsilon_0$ and $\sigma_2 = 0.4$ S/m [3], and the penetration depth for this soil is 0.06 m. The rms error of the reconstructed shape function is 13%. This result is not good as compared to the case of sandy soil because the penetration depth of the loamy soil is smaller than that of the sandy soil. It would be necessary to use lower frequency for the loamy soil in order to reduce the attenuation.

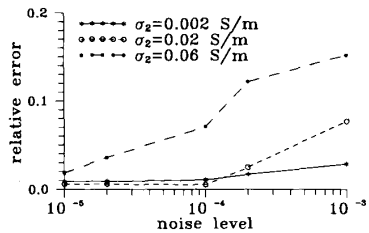

Fig. 6. Reconstruction error as a function of noise level at a burying depth of $a = 2\lambda_0$ for object A in three different soils.

IV. Conclusions

We have applied the Newton–Kantorovitch algorithm to reconstruct the shape of a perfectly conducting object buried in a lossy half-space (soil) by the knowledge of the scattered field measured in another half-space (air). The nonlinear integral equations have been transformed into matrix forms by the Newton–Kantorovitch technique and moment method. Numerical simulations concerning the shape of the object have been carried out for various burying depths, soil conductivities, and additive random noise. It has been found that the image quality greatly depends on the soil parameters and burying depth.

References

[1] L. C. Chan, L. Peters, and D. L. Moffatt, "Improved performance of a subsurface radar target identification system through antenna design," *IEEE Trans. Antennas Propagat.*, vol. AP-29, pp. 307–311, Mar. 1981.

[2] N. Osumi and K. Ueno, "Microwave holographic imaging of underground objects," *IEEE Trans. Antennas Propagat.*, vol. AP-33, pp. 152–159, Feb. 1985.

[3] L. Chommeloux, C. Pichot, and J. C. Bolomey, "Electromagnetic modeling for microwave imaging of cylindrical buried inhomogeneities," *IEEE Trans. Microwave Theory Tech.*, vol. MTT-34, pp. 1064–1076, Oct. 1986.

[4] C. C. Chiu and Y. W. Kiang, "Inverse scattering of a buried conducting cylinder," *Inverse Problems*, vol. 7, pp. 187–202, Apr. 1991.

[5] A. Roger, "Newton-Kantorovitch algorithm applied to an electromagnetic inverse problem," *IEEE Trans. Antennas Propagat.*, vol. AP-29, pp. 232–238, Mar. 1981.

A Self-Steering Array for the SHARP Microwave-Powered Aircraft

Thomas W. R. East

Abstract—**SHARP is a proposed airborne platform consisting of a light aircraft powered by microwave energy beamed to it from the ground. This paper describes a novel design for a phased array which automatically tracks the aircraft as it flies on station. It uses a feedback link through the transmitted beam. Computer simulations are presented.**

I. Introduction

SHARP (Stationary High Altitude Relay Platform) is an airborne platform to be used for communications or other purposes, proposed by, and under development at, the Canadian Department of Communications [1], [2]. It would fly on station at an altitude of about 21 km (69 000 ft) above the strongest winds. Its propeller would be turned by an electric motor of about 1 kW, which receives its power from an antenna on the underside of the aircraft, and which intercepts microwave radiation transmitted from the ground. This antenna, known as a rectenna, consists of an array of dipoles, each with its own rectifier, so that it is essentially nondirectional [3]–[5].

Brown demonstrated powering of a tethered helicopter by microwave transmission [6].

A small-scale model of the SHARP proposed system has been successfully flown out of doors at a height of several tens of meters for several minutes, powered solely by a microwave beam from a parabolic antenna at the ground, at the Department of Communications Laboratory near Ottawa, Canada.

A suitable frequency band for such a system is the microwave heating band, 2450 MHz ± 1%. In a full-scale system, to achieve an acceptable efficiency of power transmission, the beam must be focused down to a narrow spot, not much larger than the aircraft itself. This requires that the ground antenna have a large aperture, best achieved by an array laid flat on the ground. It turns out that the transmitting array would be considerably larger than the rectenna. On the other hand, to keep on station, in light winds, the aircraft will have to fly in a circle with a radius several times the size of the rectenna. This means that the ground array must have some steering capability, and that the beam should focus on and follow the target.

The individual antennas can consist of parabolic reflectors, each steered to follow the aircraft (Fig. 1). This paper addresses the problem of phasing the antennas to combine constructively at the rectenna. Alternatively, the array can consist of individual radiators or fixed groups of radiators: the phasing system proposed here would apply equally and would form and steer the beam.

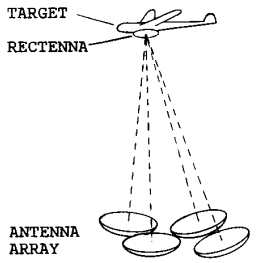

Fig. 1. SHARP system.

The prior art for solving this problem includes the conventional method (applicable to all phased arrays) and the retrodirective array, which both have disadvantages, and beam tagging, which is the basis for the ideas presented in this communication.

A. Conventional Phased Array Technique

This well-known approach (see, for example, [7]) is to feed the elements from a common source of carrier (the RF exciter) through equivalent cable lengths to form a boresight beam, and then to apply calculated phase shifts to each element in analog [8] or digital [9] phase shifters to allow for the off-boresight angle of the target. Even to achieve the boresight beam may require an extensive calibration procedure, which must be repeated periodically to correct for temperature and other disturbing effects. Then to aim the beam at the target requires a calculation of phase shift for each antenna, to be repeated as the target moves. In a SHARP system, a parallel beam is not the optimum: for maximum efficiency, the beam must converge on the vehicle.

B. The Retrodirective Array

The target vehicle carries a beacon which radiates a test signal, which is received by the array on the ground. The phase of the received signal at each antenna is measured relative to the phase of a signal distributed to all antennas, and the result is used to adjust the antenna phase shifter. (See [10], for example.)

All "retrodirective arrays" use either time-division multiplexing (shutting off the main transmission while the test signal is received on the same frequency) or frequency-division multiplexing (the test transmission is on a different frequency from the main transmission). Both have disadvantages, the main ones being the fact that every element has to have a receiver, and the need to distribute a phase standard.

C. Beam Tagging

Adams [11] has described a method (called "beam tagging") of applying low-index phase modulation to one of two antennas aimed at the same target, and measuring resultant amplitude modulation to correct the phase alignment between them. O'Meara [12] used this technique for phase-aligning lasers onto a target. Shrader [13] and Gray [14] applied this method to testing a large radar array.

Manuscript received June 20, 1991; revised June 16, 1992.

The author is with Tom East Engineering Services, Waterloo, Ont., Canada N2L 4N3.

IEEE Log Number 9204907.

0018-926X/92$03.00